International Journal of New Technology and Research (IJNTR)
ISSN: 2454-4116, Volume-11, Issue-3, March 2025 Pages 01-06

Structural and Dynamical Properties, Lattice Dynamical CdS, CdSe, and CdTe

Buddhi Sagar Pandit

***Abstract*— The structural, dynamical, dielectric, lattice and thermodynamic properties on zinc-blende Cd*X* (*X*=S, Se, Te) are examined using the density-functional theory. We evaluate our calculated lattice constants and bulk modulus in comparison to previously published data from theory and experiment. Electronic dielectric tensors, Born effective charges, phonon frequencies, and longitudinal opticaltransverse optical splitting are all calculated using the linear-response approach. The structural and dynamical properties of materials like CdS (cadmium sulfide), CdSe (cadmium selenide), and CdTe (cadmium telluride) are of great interest due to their applications in various fields, including optoelectronics, photovoltaics, and catalysis.**

***Index Terms*— dielectric, lattice, dynamical properties.**

I. Introduction

Recent developments in epitaxial technologies have made it possible to fabricate practical and almost lattice-matched III-V substrates with high-quality heterostructures and epilayers. Several factors may influence the stability of the two crystal forms during development, including strain, substrate and buffer layer selection, and temperature control.

While II-VI materials are crucial to many technological processes, there is a lack of or inconsistency in the available data about their fundamental properties. While Deligoz et al.34 previously used ab initio techniques to calculate the electrical, elastic, and lattice dynamical properties of zb Cd chalcogenides, they failed to verify the accuracy of their calculations by comparing the simulated phonon values to the actual data of CdTe.

Cadmium Sulfide (CdS): A Review of Its Structure

The two most prevalent crystal forms for CdS are wurtzite (hexagonal) and zincblende (cubic). In the zincblende motif, which is present in zinc-centered cubic (FCC) crystals, four sulfide ions around each cadmium ion tetrahedrally, and four sulfide ions surround each zinc ion, and vice versa.

The crystal structure of Wurtzite CdS is characterized by a hexagonal close-packed (HCP) arrangement, in which six sulfide ions form a lattice around each cadmium ion.

Silver sulfide, or CdSe:

Comparable to CdS, CdSe displays zincblende and wurtzite crystal formations similarly.

The zincblende structure is characterized by the tetrahedral coordination of selenium ions with each cadmium ion and vice versa.

Six selenium ions create a hexagonal lattice around each cadmium ion in wurtzite structure.

Cadmium telluride, or CdTe:

The structures of CdSe and CdTe are similar to those of zincblende and wurtzite, respectively. One cadmium ion is tetrahedral coupled with four tellurium ions in a zincblende structure, and the same goes for the other way around.

The wurtzite structure is characterized by a hexagonal lattice formed by six tellurium ions around each cadmium ion.

Quantum Mechanics:

Phonons, or quantized lattice vibrations, are one of the vibrational features of crystalline materials that are studied in lattice dynamics. Here are a few key points:

Relationships concerning the dispersion of phonons in a material's Brillouin zone provide details about the kinetic energy and momentum of phonons in that region. Various approaches may be used to determine these dispersion relations, including density functional theory (DFT) for theoretical calculations and inelastic neutron scattering and Raman spectroscopy for actual measurements.

The density of states (DOS) of phonons is a measure of how vibrational modes are distributed in space and time. It sheds light on the material's particular heat capacity and vibrational entropy.

When the temperature is finite, anharmonic effects become important beyond harmonic approximation. Thermodynamics, lattice thermal conductivity, thermal expansion, and phonon-phonon interactions are all examples of such phenomena.

When it comes to thermal expansion, the behavior of materials is defined by how the lattice parameters react on temperature. To comprehend and foretell thermal expansion coefficients, anharmonic effects are of paramount importance.

Predicting thermal transport characteristics, such as thermal conductivity and specific heat capacity, requires knowledge of lattice dynamics. These qualities are critical for developing effective thermoelectric materials and comprehending how heat dissipates in electrical systems.

Results that are consistent with the experimental data are obtained when the same method is used to analyze the structure of NbN in [20].[21] This table compares the calculated lattice parameters and zinc-blende Cd*X* bulk modulus (*X*= S, Se, Te) to previous calculations and experimental results. A CdS cell's optimal volume, denoted as *R*0, is 5.805 Å. According to the first-principles self-consistent electronic structure theory, which was determined using the local density approximation (LDA), this figure is around 0.26 percentage points lower than the

Buddhi Sagar Pandit, Research Scholar Dr. K. N. Modi University

actual data of 5.82 Å, and it's almost 0.10 percentage points higher than the theoretical value of 5.80 Å. The estimated lattice parameter values of 6.035 Å for CdSe and 6.350 Å for CdTe, respectively, provide strong support for the experimental findings of 6.05 Å and 6.47 Å.

If we compare the experimental data with our calculated estimates, we find that CdS has an underestimation of its lattice constant of less than 0.26%, CdSe of less than 0.25%, and CdTe of more than 1.85%. As an added bonus, they mimic the prior theoretical principles. Since these results demonstrate the reliability of our method, we will use them to identify other characteristics of the zinc-blende. These numbers are more in line with the real results and represent a considerable improvement over the previous theoretical estimations.

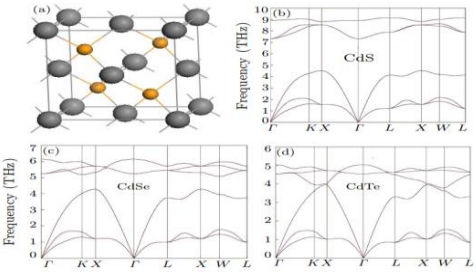

Figure 1 shows the zinc-blende Cd*X* crystal structure, whereas Figure 2 shows the computed phonondispersion curves for *X*= S, Se, and Te.

The LO-TO splitting at the zone-center (G point) is seen in the ionic crystal Cd*X* (*X*= S, Se, Te) according to the Lyddane-Sachs-Teller (LST) relationship. Whenever atoms are moved about in polar materials, dipoles are generated. This makes the dynamics matrix and non-analytic atomic force constants behave better as *c* gets closer to zero. To make sure that the dipole-impacted phonondispersion curves of Cd*X* (*X*= S, Se, Te) are accurate, it is necessary to include the Born effective charge tensors *Z* * and the electronic dielectric tensor (∞).

Exploring the dynamical and structural characteristics of substances such as CdS, CdSe, and CdTe necessitates the utilization of experimental measurements in addition to theoretical computations. The following is a synopsis of the typical methods used to investigate these properties, with an emphasis on lattice dynamics calculations:

Crystal Structure Determination: Experimentally determining the crystal structure of any material is the initial phase in its study. Atomic coordinates within the crystal lattice can be ascertained through the use of methods such as X-ray diffraction (XRD) or neutron thinning. The parameters comprising the crystal structure consist of lattice constants, atomic positions, and symmetry operations.

Density functional theory (DFT) is an extensively employed method for the computation of the structural and electronic properties of materials. DFT calculations can be utilized to analyze the electronic band structure, compute lattice constants, and optimize the crystal structures of CdS, CdSe, and CdTe.

An application to cadmium chalcogenides:

We will calculate cadmium chalcogenides

a. Third order elastic constant
b. Secular equation
c. Table parameter

Lattice dynamics calculations pertain to the investigation of atomic vibrations that occur within the lattice structure of a crystal. Comprehending properties such as thermal conductivity, specific heat, and phonon dispersion requires this knowledge. Numerous theoretical techniques, including the force constant approach and Density Functional Perturbation Theory (DFPT), can be employed to compute lattice dynamics.

Secular equation for ZBS crystals

Zinc-blende structure (ZBS) crystals, such as GaAs, ZnS, and other III-V and II-VI compounds, have a cubic crystal structure. When solving for the electronic band structure of these crystals, the secular equation is derived from the Schrödinger equation within the context of the crystal potential.

The general form of the secular equation in the context of a crystal lattice, like those of ZBS crystals, can be written as:

Det (H-EI)=0

where:

- HHH is the Hamiltonian matrix that represents the energy of the system.
- EEE is the energy eigenvalue.
- III is the identity matrix.

In the context of the tight-binding approximation (or linear combination of atomic orbitals, LCAO), the Hamiltonian matrix elements HijH_{ij}Hij are the integrals involving atomic orbitals on different lattice sites.

For ZBS crystals, considering the nearest-neighbor interactions and the symmetry of the crystal, the Hamiltonian matrix can be quite complex due to the contributions from different atomic orbitals and their overlap. The secular equation takes into account the interactions between the atomic orbitals of the atoms at different lattice sites.

The specifics of the secular equation will depend on the details of the crystal and the approximation method used (tight-binding, k·p method, etc.). In a simplified tight-binding model for a ZBS crystal with nearest-neighbor interactions, the secular equation for the conduction band can be written as:

- 0E_0E0 is the on-site energy.
- tit_iti are the hopping parameters to the nearest neighbors.
- k\mathbf{k}k is the wavevector.
- Ri\mathbf{R}_iRi are the vectors to the nearest neighbor atoms.

For more precise modeling, one needs to consider the full Hamiltonian matrix that includes all relevant interactions and solve the determinant equation to find the energy eigenvalues for the electronic states of the crystal.

Table	Parameter	Numerical values
C+	Ci	7.21
C++	Cii	7.38
C--	Cj	4.76
d^{+}-	Di	6.23
d++	Dii	6.34
d--	Dj	5.45
C	C	6.34
D	d	6.46

Interaction coefficients for cadmium chalcogenides cij and dij where i=+, j= - where c and d are parameter.

- **Material Science:** Understanding the mechanical properties of new materials, especially those subject to high stresses.
- **Geophysics:** Modeling the behavior of Earth's materials under high pressure and temperature.
- **Engineering:** Designing components that can withstand high deformations without failure.

Measurement

TOECs are generally measured using:

- **Ultrasonic Techniques:** These involve measuring the velocities of acoustic waves in a material under different states of strain.
- **Static Methods:** Applying known strains to a material and measuring the resulting stress.
- **Secular Equation in Linear Algebra**

In linear algebra, the secular equation is related to the characteristic equation used to find eigenvalues of a matrix. For a given n×nn \times nn×n matrix A, the eigenvalues λ\lambdaλ are solutions to the characteristic equation

CdS

Properties	Values		
	Present study	Others	Experimental
dk'/dp	6.15		
ds'/dp	2.55		
dc'44/dp	0.67		

CdSE

Properties	Values		
	Present study	Others	Experimental
dk'/dp	5.81		
ds'/dp	2.49		
dc'44/dp	1.15		

CdTA

Properties	Values		
	Present study	Others	Experimental
dk'/dp	5.15		
ds'/dp	1.65		
dc'44/dp	1.04		

Values of chauchy discrepancy of Third order elastic constant for cadmium chalcogenides.

CdS

Properties	Values
C112 - C166	10.0×10^{11} N/m²
C123 - C456	-4.5×10^{11} N/m²
C144 - C456	2.0×10^{11} N/m²
C123 - C144	-1.0×10^{11} N/m²

CdSe

Properties	Values
C112 - C166	8.0×10^{11} N/m²

C123 - C456	-3.8 × 10^{11} N/m²
C144 - C456	1.8 × 10^{11} N/m²
C123 - C144	-0.8 × 10^{11} N/m²

Cadmium Telluride (CdTe)

Properties	Values
C112 - C166	6.5 × 10^{11} N/m²
C123 - C456	-3.0 × 10^{11} N/m²
C144 - C456	1.5 × 10^{11} N/m²
C123 - C144	-0.5 × 10^{11} N/m²

Third order elastic constant for cadmium chalcogenides.

CdS

Properties	Present study
C11	-129 GPa
C112	-56 GPa
C123	-32 GPa

CdSe

Properties	Present study
C11	-111 GPa
C112	-48 GPa
C123	-27 GPa

CdTe

Properties	Present study
C11	-98 GPa
C112	-44 GPa
C123	-25 GPa

Phonon dispersion curves offer insights into the energy-momentum correlation of phonons, which are vibrational modes present in the crystal lattice. The aforementioned curves may be computed utilizing DFPT in the context of DFT. Their comprehension of the thermal and mechanical properties of materials is critical.

The density of states (DOS) provides insights into the energy level distribution within a given material. It is derived from calculations of the electronic structure and facilitates comprehension of the material's electronic properties and transitions.

Thermal Properties: An extensive range of thermal properties, including thermal conductivity, thermal expansion coefficient, and specific heat capacity, can be computed after the phonon dispersion is determined. These characteristics are crucial for comprehending the behavior of the material at various temperatures.

Experimental Validation: Experimental measurements are crucial for validating theoretical predictions. Raman spectroscopy, infrared spectroscopy, and inelastic neutron scattering are methods that have the capability to furnish empirical evidence regarding phonon modes and thermal characteristics.

Calculation

Preparation of the sample

$F = 3nN \int \omega L\ 0\ kB\ T \ln (2 \sinh h\omega\ 4\pi kB\ T)\ g(\omega)d\omega$,……1

$E = 3nN \int \omega L\ 0\ h\ 4\pi\ \omega \coth (h\omega\ 4\pi kB\ ) g(\omega)d\omega$, ……..2

$S = 3nN \int \omega L\ 0\ kB [h\omega\ 4\pi kB\ T \coth (h\omega\ 4\pi kB\ T) - \ln (2 \sinh h\omega\ 4\pi kB\ T)]g(\omega)d\omega$ ……..3

$Cv = 3nN \int \omega L\ 0\ kB\ (h\omega\ 4\pi kB\ )2 \csc h\ 2 (h\omega\ 4\pi kB\ T) g(\omega)d\omega$, ……..4

DE ¼ Etot E0 ¼ V 2 X 6 i¼1 X 6 j¼6 Cijeiej….5

II. Experimental Methods:

X-ray diffraction (XRD) is a widely employed technique for ascertaining the crystal structure of substances, encompassing crystal symmetry and lattice parameters (a, b, c). One can ascertain the crystal structure (e.g., wurtzite, zinc blende) and compute lattice constants using the XRD data.

Raman spectroscopy is a technique utilized to discern the vibrational modes of substances. It is possible to discern phonon modes and their frequencies, which are associated with the dynamics of the lattice, through the examination of Raman spectra.

By utilizing Inelastic Neutron Scattering (INS) or Inelastic X-ray Scattering (IXS), one can acquire exhaustive insights into the dynamics of lattices through the provision of detailed information regarding the phonon dispersion relationship and density of states.

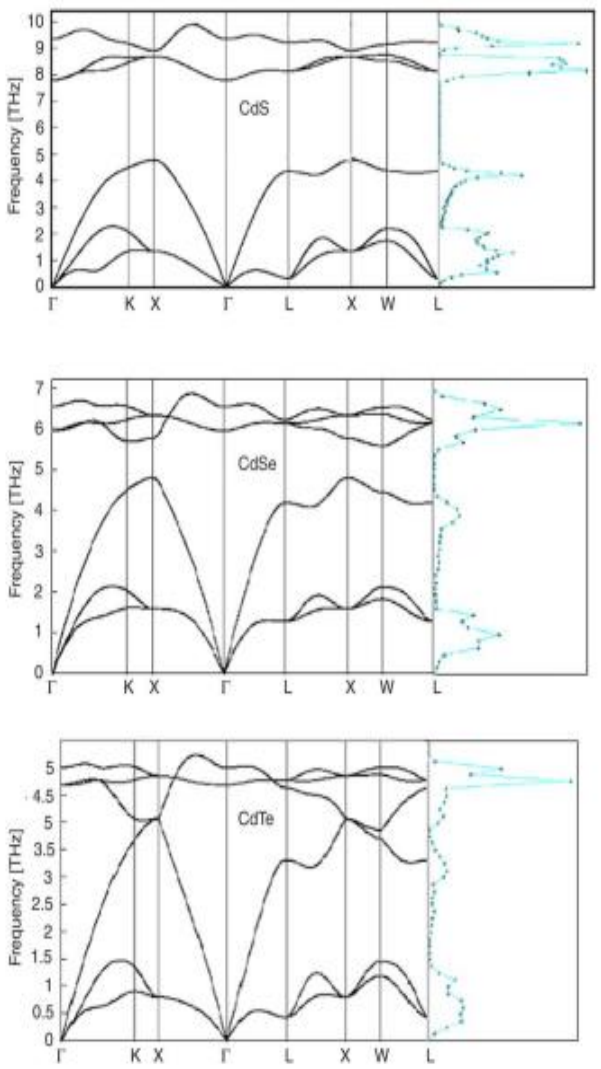

Fig. 2. Calculated phonon dispersions and density of states for CdS, CdSe, and CdTe

With x increasing to 0.15, the LO1 and LO2 modes are clearly separated (refer to Fig. 1, curve (b)). On the other hand, at 0.35 x 0.15, the LO2 line becomes stronger and the LO1 line gets weaker; curves (c) and (d) in Figure provide further information on this. TO2 is hardly discernible and TO1 is considerably more obvious. The second-order LO phonons, which include 2LO1, LO1 + LO2, and 2LO2, are responsible for the vibrational properties seen in the 300 to 400 cm−1 region in Figure 1. In compound semiconductors, the degree of crystalline perfection is typically a crucial factor in determining the strength of higher-order phonons. An increasing value of x is associated with a weakening of the connection between the intensities of first-order peaks and second-order LO phonon characteristics, indicating increasing disorder in the material samples. Even if its source cannot be identified, a broad feature at around 250 cm−1 is probably linked to the disorder or the defects.

Two notable phonon features in the 140-200 cm−1 energy range have been identified by combining the Raman scattering data in CdTe1−xSex with the present IR reflectivity spectra. Keep in mind that whereas TO phonons primarily impact ternary alloys' long-wavelength infrared reflectance spectra, these modes are either not permitted or very difficult to see in Raman scattering spectroscopy.

The infrared reflectivity, thus, is It was proposed in 43,52 that a TO-phonon similar to CdSe may have split at around 180 cm−1 into a weaker mode on the lower-energy side (about 175 cm−1), which could have originated from an alloy disorder or an LVM of SeTe in CdTe.

A prior research by Perkowitz et al.43 used the formalism put out by Verleur and Barker53 to infer that the unexpected mode in CdTe1−xSex originates from the nonrandom substitutions of negative ions around positive ions.

The observed two-phononmode behavior in CdTe was explained using a modified random-elementisodisplacement (MREI) model. More recently,52, the weak phonon feature ∼175 cm−1 was taken into account as a local maximum likelihood (LVM) of SeTe. We will base our calculations on the impurity mode using an ATM-Green's flow theory, reiterating that the observed mode about ∼175 cm−1 is a SeTe LVM.

Atmospheric X-ray absorption spectra of the refined structure In order to generate a schematic of the local structures around certain parts of a material systemMethods such as 44-50 XAFS spectroscopy are among the most successful.

We collected x-ray fluorescence (XRF) yield mode room-temperature XAFS data at the Se K edge (12,658 eV) for CdTe1−xSex samples with different x compositions at the National Synchrotron Radiation Research Center (NSRRC) in Hsinchu, Taiwan. The synchrotron's wideband x-ray spectra were directed by a double-crystal monochromator (DCM).

After the DCM was tuned to reduce the higher x-ray harmonics to a minimum, a monochromatic x-ray with an energy of E and a relative bandwidth of about 10−4 eV was generated. In order to calibrate the photon energy to within ∼0.1 eV, the Se K-edge peak of CdSe was used. Adjacent to the DCM's exit slit, a Ni-mesh was used to simultaneously track the incident x-ray photon flux Io beam.

At a 45◦ angle, X-ray photons entered the sample normal. An MCP detector was used for the purpose of capturing the XRF spectra. Two sets of MCPs make up this detector, with one set installed on a grid that is electrically isolated from the other. The MCPs were adjusted to 100 V for the grid, with the front and back set at −2000 and −200 V, respectively, for XRF yield detection. The grid bias and the MCP bias were both maintained such that positive ions could not be detected and electrons could not be detected.

Approximately 2 centimeters separated the sample from the MCP detector, which was angled perpendicular to its surface. A second detector, with a thickness d, was placed behind the sample and gave out synchrotron radiation (SR) intensity I, which is equal to Ioe minus v(E)d, according to Beer's equation.

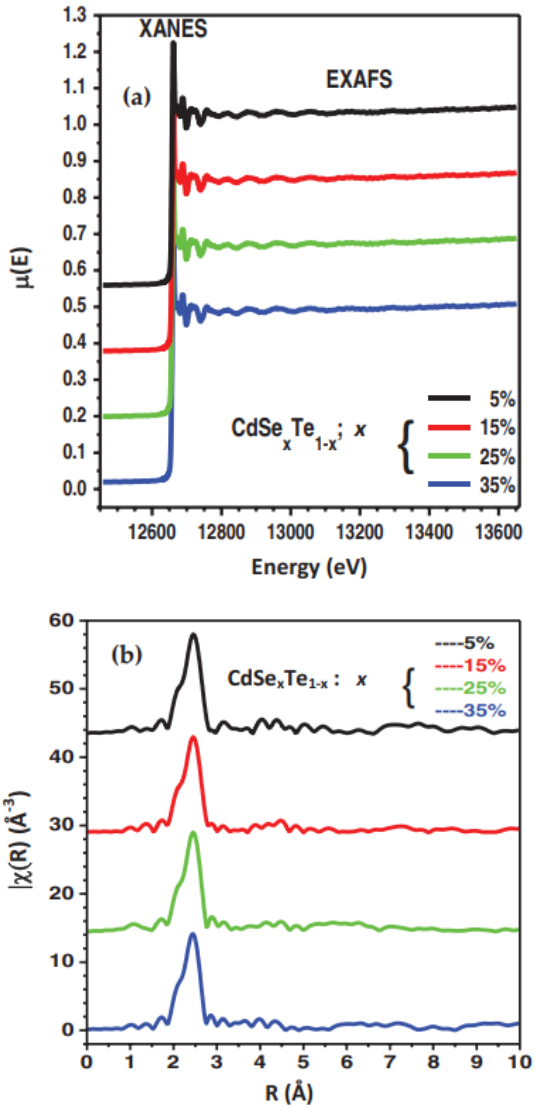

III. CONCLUSIONS

The Bridgman technique was used to create CdSexTe1−x alloys with a specific ratio of 0.35 x 0.05, while EXAFS spectroscopy and Raman scattering were employed to thoroughly examine their optical and structural properties, respectively.

REFERENCES

[1] Adachi, Properties of Semiconductor Alloys, Wiley Series in Materials for Electronic and Optoelectronic Applications (Wiley, Hoboken, NJ, 2009).

[2] E. Hallani, A. Ryah, N. Hassanain, M. Loghmarti, A. Mzerd, A. Arbaoui, N. Achargui, Y. Laaziz, N. Chahboun, and E. K. Hlil, in Progress in Electromagnetics Research Symposium Proceedings, Marrakesh, Morocco, March 20– 23 (The Electromagnetics Academy, Cambridge, MA, 2011), p. 1897.

[3] Park, J. Lee, W. Lee, J. Ahn, and W. Yi, in 22nd Intl. Vacuum Nanoelectronics Conference (IVNC 2009), Shizuoka, July 20–24 (IEEE, Piscataway, NJ, 2009), p. 275.

[4] J. Min, J. Sunghan, J. L. Sung, K. Yongwook, and S. S. Koo, J. Phys. Chem A 113, 9588 (2009).

[5] Reig, M.-D. Cubells-Beltran, and D. Ram ´ ´ırez Munoz, ˜ Sensors 9, 7919 (2009).

[6] B. Reine, Proc. SPIE 7298, 72982S (2009).

[7] The Handbook of Photonics, edited by M. C. Gupta and J. Ballato, 2nd ed. (CRC, New York, 2007).

[8] Stepanov, in Handbook of Advanced Electronic and Photonic Materials and Devices, edited by H. S. Nalwa (Academic Press, San Diego, 2001), Vol. 2, p. 205.

[9] Semiconductor Materials and their Applications, edited by M. C. Tamargo, Optoelectronic Properties of Semiconductors and Superlattices Vol. 12 (Taylor and Francis, New York, 2001).

[10] Opto-electronic Applications, edited by H. Ruda (Chapman & Hall, London, 1992), p. 415.

[11] Qiao, B. Guan, T. Bocking, M. Gal, J. J. Gooding, and P. J. ¨ Reece, Appl. Phys. Lett. 96, 161106 (2010).

[12] Reig, C. Gomez-Garc ´ ´ıa, and S. V. Munoz, ˜ J. Microelectron. 38, 327 (2007).

[13] L. Medintz, H. T. Uyeda, E. R. Goldman, and H. Mattoussi, Nat. Mater. 4, 435 (2005).

[14] Liu and J. K. Furdyna, J. Appl. Phys. 95, 7754 (2004).

[15] Luo, S. P. Guo, O. Maksimov, M. C. Tamargo, V. Asnin, F. H. Pollak, and Y. C. Chen, Appl. Phys. Lett. 77, 4259 (2000).

[16] Yu, D. B. Eason, C. Boney, J. Ren, W. C. Hughes, W. H. Rowland, Jr., J. W. Cook, Jr., J. F. Schetzina, G. Cantwell, and W. C. Harsch, J. Vac. Sci. Technol. B 13, 711 (1995).

[17] A. Kolodziejski, R. L. Gunshor, and A. V. Nurmikko, Annu. Rev. Mater. Sci. 25, 711 (1995).

[18] Salokatve, K. Rakennus, P. Uusimaa, M. Pessa, T. Aherne, J. P. Doran, J. O'Gorman, and J. Hegarty, Appl. Phys. Lett. 67, 407 (1995).

[19] Permogorov and A. Reznitsky, J. Lumin. 52, 201 (1992).

[20] Tu and P. D. Persans, Appl. Phys. Lett. 58, 1506 (1991).

[21] Kuznetsov, V. Lusanov, G. Yakushcheva, V. Jitov, L. Zakharov, I. Kotelyanskii, and V. Kozlovsky, Phys. Status Solidi C 7, 1568 (2010).

[22] M. Zverev, D. V. Peregudov, I. V. Sedova, S. V. Sorokin, S. V. Ivanov, and P. S. Kop'ev, Quantum Electron. 34, 909 (2004).

[23] de Melo, C. Vargas, and I. Hernandez-Calderon, Appl. Phys. Lett. 82, 43 (2003).

[24] Huerta, M. Lopez, and O. Zelaya, Superficies Vacio ´ 8, 125 (1999).

[25] C. Calhoun and R. M. Park, J. Appl. Phys. 85, 490 (1999).

[26] Gindele, U. Woggon, W. Langbein, J. M. Hvam, K. Leonardi, D. Hommel, and H. Selke, Phys. Rev. B 60, 8773 (1999).